Supporting Information

In situ tetrazole templated chair-like decanuclear azido-cobalt(II) SMM containing both tetra- and octa-hedral Co(II) ions

Yuan-Zhu Zhang,[*,a,b] **Song Gao**[a]**, Osamu Sato,**[*,b]

[a] *Beijing National Laboratory for Molecular Sciences, State Key Laboratory of Rare Earth Materials Chemistry and Applications, College of Chemistry and Molecular Engineering, Peking University, 100871 Beijing, China. Fax: (+86)-10-62751708; Tel: (+86)-10-62756320; E-mail: gaosong@pku.edu.cn*
[b] *Institute for Materials Chemistry and Engineering, Kyushu University, 6-1 Kasuga, 816-8580, Fukuoka, Japan; Fax & Tel: (+81)92-583-7787; E-mail: sato@cm.kyushu-u.ac.jp*

Experimental Section

Materials and Physical Measurements.

All starting materials were commercially available, reagent grade and used as purchased without further purification. Elemental analysis of carbon, hydrogen, and nitrogen were carried out with an Elementary Vario EL. The IR spectra were recorded against pure samples on a Magna-IR 750 spectrophotometer in the 4000-500 cm^{-1} region. The measurements of variable–temperature magnetic susceptibility, ac magnetic susceptibility and field-dependence of magnetization were performed on a Quantum Design MPMS XL-5 SQUID magnetometer. The experimental susceptibilities were corrected for the diamagnetism (Pascal's tables).

Caution! Perchlorate salts of metal complexes with organic compounds are potentially explosive. Only a small amount of material should be prepared and handled with great care.

Single Crystal structural data:

The diffraction data collection of **1** was made at 110(2) K on a Bruker APEX diffractometer equipped with a CCD detector. Initial cell parameters were obtained (DENZO) from ten 1º frames (SCALEPACK). The data sets were recorded as ϖ-scans at 1.0° step width. Integration was performed with the Bruker SAINT software package and absorption corrections were empirically applied using SADABS. The crystal structure was solved by the direct method (SHELXS-97) and refined by full-matrix least squares (SHELXL-97) on F² and

empirical absorption corrections (SADABS) were applied. All non-hydrogen atoms were located by alternating cycles of least squares refinements and difference Fourier maps. All hydrogen atoms were placed at calculated positions. Anisotropic thermal parameters were added for all non-hydrogen atoms.

Table S1. Crystallographic data for **1** at 110(2) K.

Compound	**1**
crystal color	Dark red
formula	$C_{104}H_{100}Co_{10}N_{70}O_{15}$
formula wt	3159.84
crystal system	Triclinic
space group	P-1
wavelength, Å	0.71073
Temperature, K	110 (2) K
a, Å	13.565(9)
b, Å	16.584(11)
c, Å	18.065(12)
α, deg	63.652(7)
β, deg	76.183(7)
γ, deg	83.562(8)
V, Å³	3536(4)
Crystal size	$0.11 \times 0.10 \times 0.06$
D_c, g cm⁻³	1.484
Z	1
μ, mm⁻¹	1.222
F(000)	1604
Measured refl.	33924
unique refl.	12420
Observed refl.[a]	7533
No. of parameters	925
GooF	1.011
$R_1{}^a$	0.0636
$wR_2{}^a$	0.1651

[a] $I \geq 2\sigma(I)$: $R_1 = \sum ||F_o| - |F_c||/\sum|F_o|$, $wR_2 = \{\sum[w(F_o{}^2 - F_c{}^2)^2]/\sum[w(F_o{}^2)^2]\}^{1/2}$.

Table S2. Selected bond distances (Å) and angles (°) for **1**.

|					
Co1-N9	2.078(5)	N9-Co1-N24ᵃ	170.5(2)	Co1ᵃ-N24-Co4	98.9(2)
Co1-N24ᵃ	2.088(5)	N9-Co1-N1	95.9(2)	Co1ᵃ-N27-Co4	98.9(2)
Co1-N1	2.088(6)	N9-Co1-N27ᵃ	90.9(2)	Co1-N9-Co2	118.0(3)
Co1-N27ᵃ	2.121(5)	N9-Co1-O1	84.6(2)	Co2-N12-Co3	117.8(2)
Co1-O1	2.143(4)	N9-Co1-N5	88.6(2)	Co3-N18-Co4	118.0(3)
Co1-N5	2.149(5)	N2-Co2-N6	168.6(2)	Co2-N9-Co5	117.9(3)
Co2-N2	2.074(6)	N2-Co2-N9	94.2(2)	Co3-N21-Co5	117.6(3)
Co2-N6	2.087(5)	N2-Co2-N15	98.0(2)	N9-N10-N11	178.9(7)
Co2-N9	2.092(5)	N2-Co2-N12	91.9(2)	N12-N13-N14	178.5(7)
Co2-N15	2.095(6)	N2-Co2-O2	76.1(2)	N15-N16-N17	176.9(10)
Co2-N12	2.108(6)	N18-Co3-N21	92.1(2)	N18-N19-N20	179.3(8)
Co2-O2	2.117(5)	N18-Co3-N12	173.9(2)	N21-N22-N23	177.8(8)
Co3-N18	2.056(6)	N18-Co3-N7	87.02(19)	N24-N25-N26	178.4(7)
Co3-N21	2.093(6)	N18-Co3-N3	91.5(2)	N27-N28-N29	178.3(7)
Co3-N12	2.098(6)	N18-Co3-O3	95.4(2)		
Co3-N7	2.109(5)	N18-Co4-N4	95.7(2)		
Co3-N3	2.107(5)	N18-Co4-N27	169.9(2)		
Co3-O3	2.125(4)	N18-Co4-N24	90.0(2)		
Co4-N18	2.062(5)	N18-Co4-N8	89.6(2)		
Co4-N4	2.086(6)	N18-Co4-O4	86.6(2)		
Co4-N27	2.090(5)	N33-Co5-N30	105.9(3)		
Co4-N24	2.122(5)	N33-Co5-N21	117.5(3)		
Co4-N8	2.147(5)	N33-Co5-N15	111.8(3)		
Co4-O4	2.184(4)				
Co5-N33	1.941(8)				
Co5-N30	1.967(7)				
Co5-N21	1.979(6)				
Co5-N15	1.993(6)				

Symmetry transformations used to generate equivalent atoms: ᵃ -x+1,-y,-z

Table S3. Fittings of Cole-Cole plots of the variable-frequency ac data, collected at 1.8 K under different dc fields (0-1500 Oe), based on a generalized Debye model.

H_{dc} / Oe	χ_s (cm³ mol⁻¹)	χ_t (cm³ mol⁻¹)	τ (S)	α	R
0	0.00000	102.80738	0.00029	0.31504	7.66×10^{-5}
250	0.00474	107.72500	0.00104	0.43970	2.46×10^{-4}
500	0.11415	94.92182	0.00328	0.45484	2.32×10^{-3}
750	0.00035	76.06037	0.00485	0.48083	1.96×10^{-4}
1000	0.00026	57.76386	0.00587	0.51972	2.11×10^{-4}
1250	0.00001	42.65962	0.00665	0.55100	1.61×10^{-4}
1500	0.00003	31.22902	0.00754	0.57912	9.78×10^{-5}
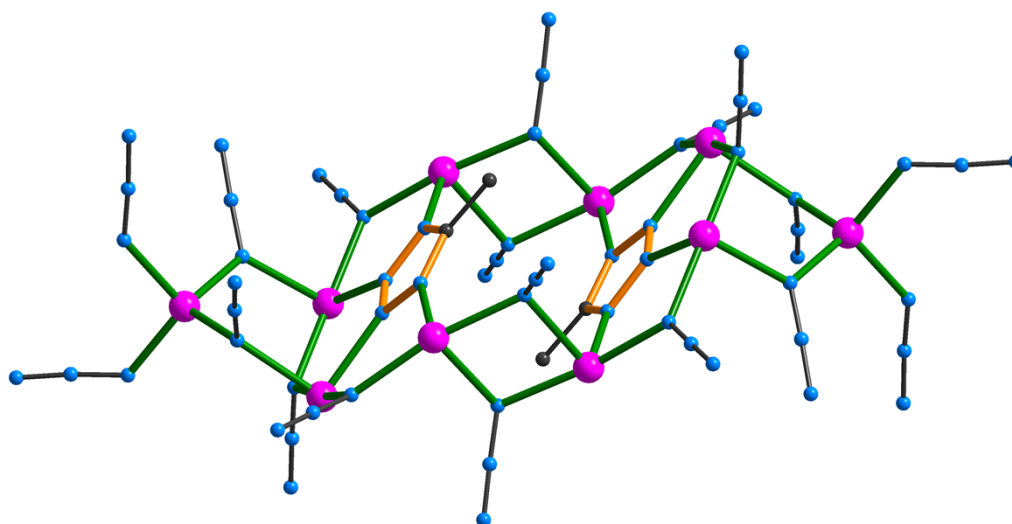
Fig. S1 View of the double-seat chair-like structure with all bzp ligands, lattice solvent and hydrogen atoms eliminated for clarity.
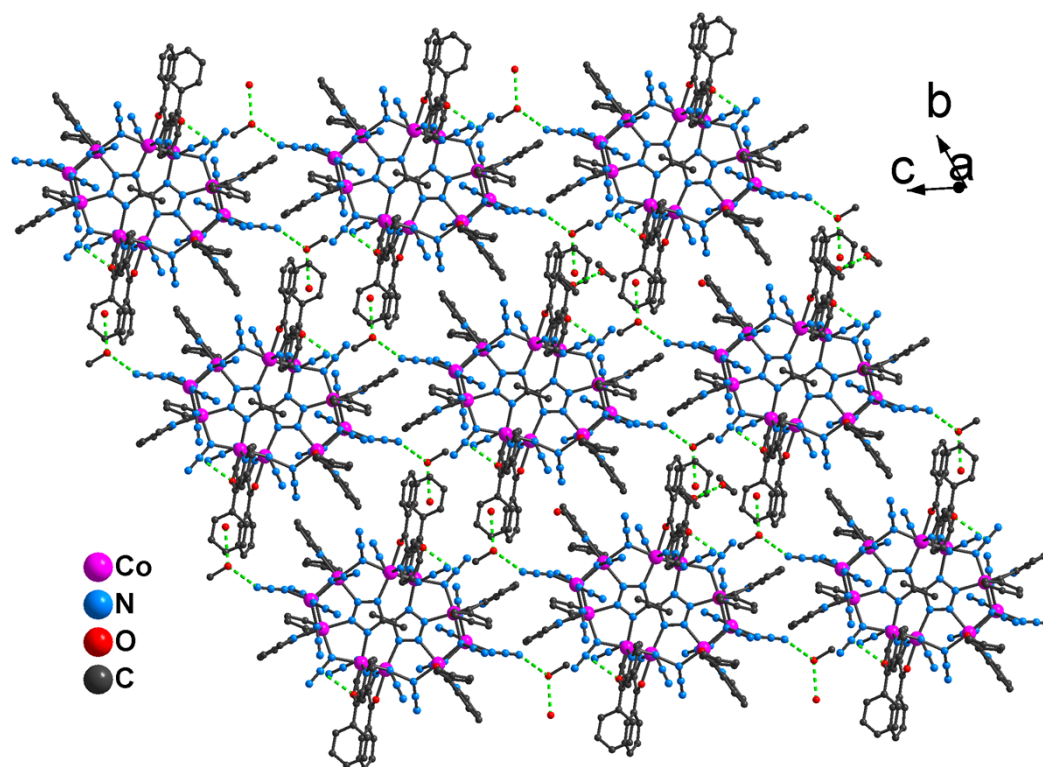
Fig. S2 Packing view of **1** showing a 3D structure, where the decanuclear $[Co^{II}_{10}]$ clusters are well isolated with the nearest intercluster Co...Co distance of 9.15(2) Å.
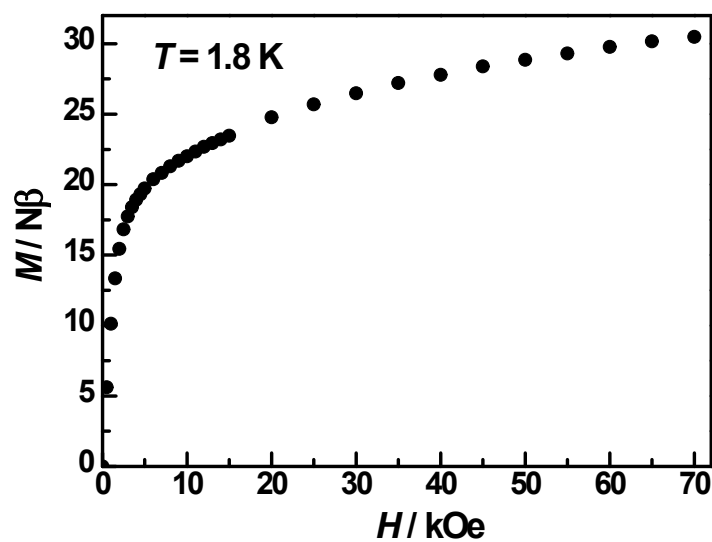
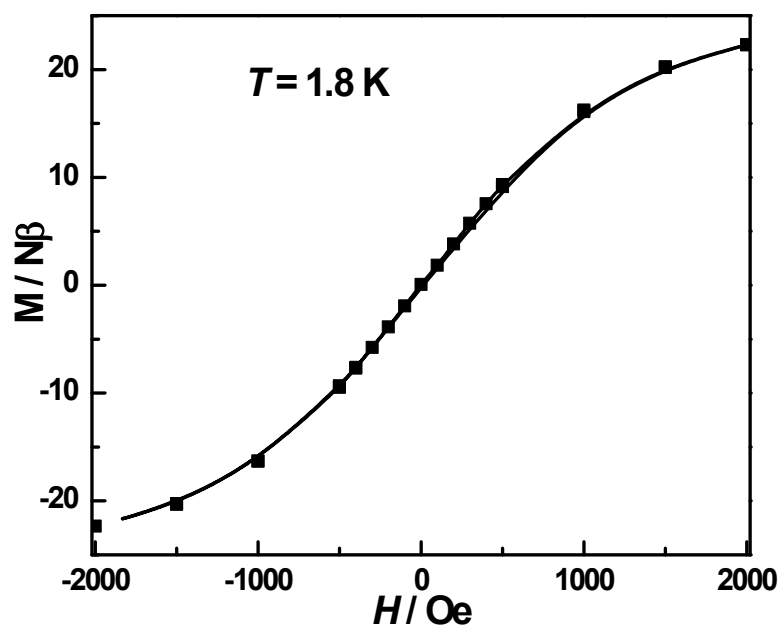**Fig. S3** Plot of isothermal dc field dependent magnetization for **1** at 1.8 K.

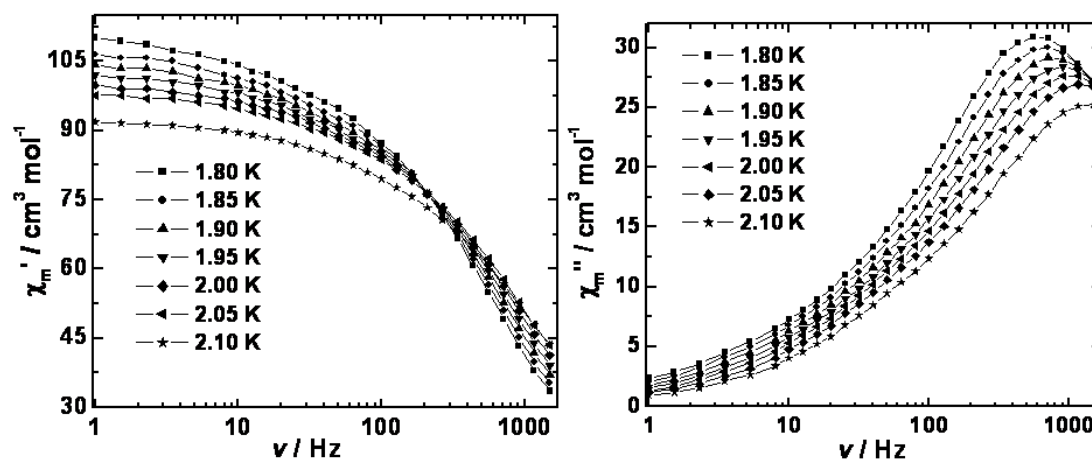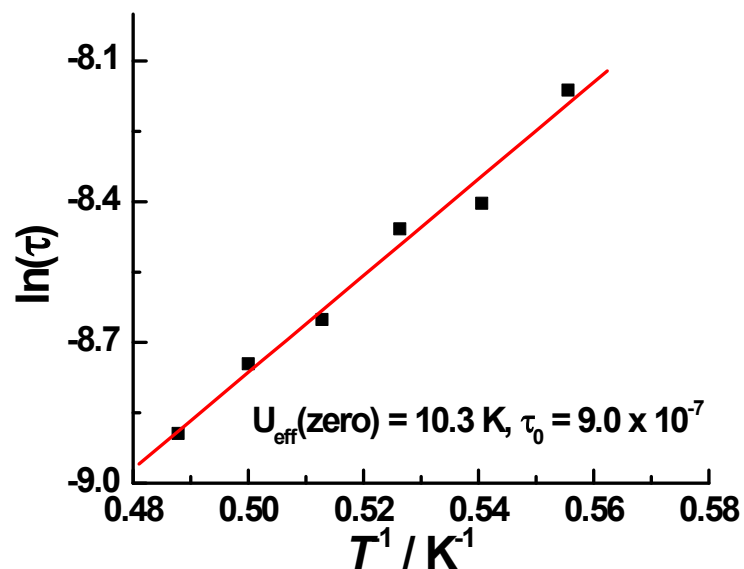**Fig. S4** Magnetic hysteresis loop at 1.8 K for **1**. Solid line is guide for eyes.

Fig. S5 Variable-frequency in-phase (χ_m', left) and out-of-phase (χ_m'', right) components of the ac magnetic susceptibility data for **1**, collected at temperatures of 1.80-2.10 K with zero dc applied field and an ac filed of 5 Oe.

Fig. S6 Arrhenius plot of relaxation time, as determined through variable-frequency ac susceptibilities at temperatures of 1.80 – 2.10 K and under an ac field of 5 Oe and zero dc field.
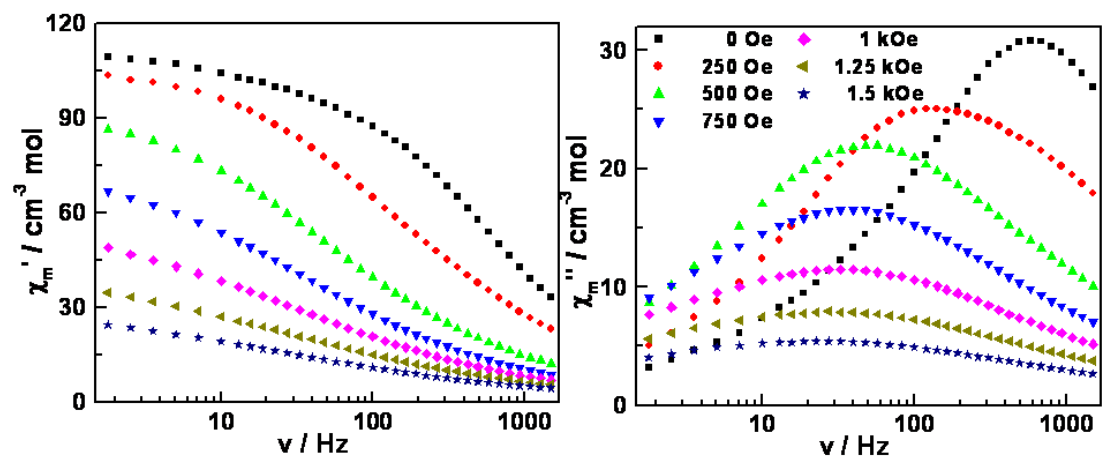
Fig. S7 Variable-frequency in-phase (χ_m', left) and out-of-phase (χ_m'', right) components of the ac magnetic susceptibility data for **1**, collected at temperatures of 1.80 K with an ac filed of 5 Oe and 0-1500 Oe dc applied fields.
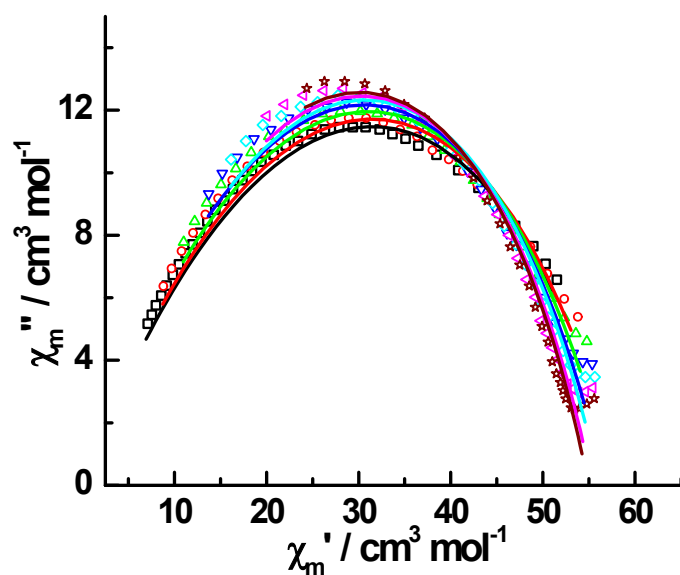
Fig. S8 Cole-Cole diagrams of **1** at 1.8 – 2.4 K with an applied dc field of 1 kOe and ac field of 5 Oe. The solid lines are least-square fittings of the data to a distribution of single relaxation processes with a generalized Debye model.[a,b]

T / K	χ_s (cm³ mol⁻¹)	χ_t (cm³ mol⁻¹)	τ (S)	α	R
1.8	0.00002	58.50841	0.00617	0.52397	2.04×10^{-4}
1.9	0.00052	58.37989	0.00334	0.51392	1.87×10^{-4}
2.0	0.00010	57.52322	0.00173	0.49809	1.64×10^{-4}
2.1	0.00075	56.73644	0.00094	0.48378	1.71×10^{-4}
2.2	0.70947	56.17240	0.00064	0.46711	1.99×10^{-4}
2.3	0.70675	55.36292	0.00035	0.45540	2.05×10^{-4}
2.4	0.73749	54.94551	0.00021	0.44693	2.13×10^{-4}

Refs: (a) Cole, K. S.; Cole, R. H. *J. Chem. Phys.* **1941**, 9, 341. (b) Aubin, S. M.; Sun, Z.; Pardi, L.; Krzysteck, J.; Folting, K.; Brunel, L.-J.; Rheingold, A. L.; Christou, G.; Hendrickson, D. N. *Inorg. Chem.* **1999**, 38, 5329.
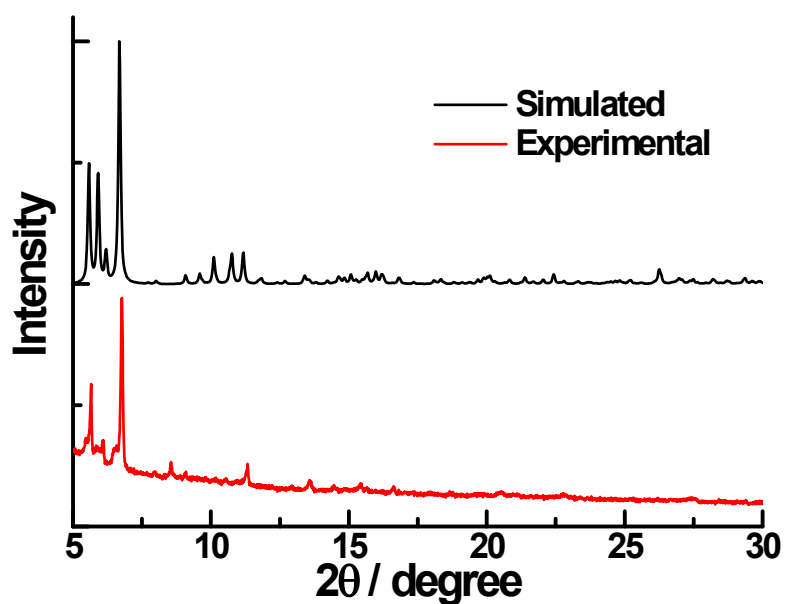
Fig. S9 Experimental and simulated powder X-ray diffraction patterns of **1**.

The powder X-ray diffraction (PXRD) data of ground fine powder (ca. 5 mg) was collected on a POWDER_SA BRUKER D8-Focus Bragg-Brentano X-ray Powder Diffractometer with Cu Kα radiation (50 kV, 30 mA) between 5.0 and 35° (2θ) at ambient temperature. Strong diffractions on PXRD spectrum well matches with those for the simulated spectrum based on the single crystal data.